Bioactive Materials 41 (2024) 1–14

Contents lists available at ScienceDirect

Bioactive Materials

journal homepage: www.keaipublishing.com/en/journals/bioactive-materials

Supragel-mediated efficient generation of pancreatic progenitor clusters and functional glucose-responsive islet-like clusters

Hongmeng Ma [a], Lilin Xu [a], Shengjie Wu [a], Songdi Wang [a], Jie Li [a], Sifan Ai [a], Zhuangzhuang Yang [a], Rigen Mo [a], Lei Lin [a], Yan Li [a], Shusen Wang [c], Jie Gao [a,**], Chen Li [b,***], Deling Kong [a,d,*]

[a] State Key Laboratory of Medicinal Chemical Biology, Key Laboratory of Bioactive Materials, Ministry of Education, and College of Life Sciences, Nankai University, Tianjin, 300071, China
[b] Tianjin Key Laboratory of Biomedical Materials, Biomedical Barriers Research Center, Institute of Biomedical Engineering, Chinese Academy of Medical Sciences & Peking Union Medical College, Tianjin, 300192, China
[c] Research Institute of Transplant Medicine, Organ Transplant Center, Tianjin First Central Hospital, Nankai University, Tianjin, China
[d] College of Life Science, Key Laboratory of Bioactive Materials (Ministry of Education), State Key Laboratory of Medicinal Chemical Biology, Xu Rongxiang Regeneration Life Science Center, Nankai University, 300071, Tianjin, China

ARTICLE INFO

Keywords:
Synthetic hydrogel
Stem cell differentiation
Mechanical stiffness
Islet clusters

ABSTRACT

Although several synthetic hydrogels with defined stiffness have been developed to facilitate the proliferation and maintenance of human pluripotent stem cells (hPSCs), the influence of biochemical cues in lineage-specific differentiation and functional cluster formation has been rarely reported. Here, we present the application of Supragel, a supramolecular hydrogel formed by synthesized biotinylated peptides, for islet-like cluster differentiation. We observed that Supragel, with a peptide concentration of 5 mg/mL promoted spontaneous hPSCs formation into uniform clusters, which is mainly attributable to a supporting stiffness of ~1.5 kPa as provided by the Supragel matrix. Supragel was also found to interact with the hPSCs and facilitate endodermal and subsequent insulin-secreting cell differentiation, partially through its components: the sequences of RGD and YIGSR that interacts with cell membrane molecules of integrin receptor. Compared to Matrigel and suspension culturing conditions, more efficient differentiation of the hPSCs was also observed at the stages 3 and 4, as well as the final stage toward generation of insulin-secreting cells. This could be explained by 1) suitable average size of the hPSCs clusters cultured on Supragel; 2) appropriate level of cell adhesive sites provided by Supragel during differentiation. It is worth noting that the Supragel culture system was more tolerance in terms of the initial seeding densities and less demanding, since a standard static cell culture condition was sufficient for the entire differentiation process. Our observations demonstrate a positive role of Supragel for hPSCs differentiation into islet-like cells, with additional potential in facilitating germ layer differentiation.

1. Introduction

The extracellular matrix (ECM) interacts with cells to regulate their behaviors during embryonic development. Matrigel, a commercially available cell culturing matrix originally derived from the Engelbreth–Holm–Swarm (EHS) tumor cells [1], has been commonly used for various organoids generation, including small intestine organoids, pancreatic acinar and ductal organoids, and liver organoids [2–5]. However, the use of Matrigel could be costly, and the inconsistencies in the biochemical and biophysical properties within-batch as well as batch-to-batch variation could also be an issue when using Matrigel for stem cell development [6,7].

Peer review under responsibility of KeAi Communications Co., Ltd.
* Corresponding author. State Key Laboratory of Medicinal Chemical Biology, Key Laboratory of Bioactive Materials, Ministry of Education, and College of Life Sciences, Nankai University, Tianjin, 300071, China.
** Corresponding author.
*** Corresponding author.
E-mail addresses: chemgaojie@nankai.edu.cn (J. Gao), cli@bme.pumc.edu.cn (C. Li), kongdeling@nankai.edu.cn (D. Kong).

https://doi.org/10.1016/j.bioactmat.2024.07.007
Received 10 April 2024; Received in revised form 19 June 2024; Accepted 4 July 2024
Available online 8 July 2024

Synthetic polymeric matrices, with defined components and the ability to precisely adjust matrix composition, molecular weight, crosslinker and the polymerization method, have been developed and could potentially provide an alternative to Matrigel [8]. Various synthetic scaffolds have been shown to exhibit similar or superior characteristics in supporting human pluripotent stem cell (hPSC) maintenance in 2D or 3D cultures than Matrigel [9–13]. Additionally, there have also been approaches to exploit the mechanical and biomedical effects of tunable synthetic matrix on stem cell differentiation [14,15]. For example, a self-assembled peptide-nanofiber hydrogel has been reported to stimulate neural stem cells to differentiate better than Matrigel [16]. It has also been shown that MMP-degradable PEG-peptide hydrogels could facilitate human MSC differentiation [17]. Similarly, a Hep-HA-MA hydrogel exhibited excellent property in supporting human ADSCs for 3D culturing and differentiation [18]. More recently, a Heparinized Gelatin-Based hydrogel was used for culturing and differentiation of hiPSC by promoting suitable cell-hydrogel interaction for definitive endoderm (DE) differentiation [19]. However, few reports have explored the role of synthetic matrix in pancreatic islet differentiation. Moreover, there remains no direct evidence examining the effects of different culturing conditions on the differentiation capacity of multipotent stem cells during insulin-secreting islet cell generation.

The pancreatic islets are the only source of insulin production, which is vital in systemic glucose management. Given the rapidly growing global diabetic population and demand for insulin, islet transplantation has emerged as the most promising approach to reverse diabetes. Generation of stem cell-derived β-cell (SC-β) clusters has attracted extensive research attention due to shortage of organ donors, a major factor that limits clinical application of islet transplantation. Several studies have successfully generated functional and mature islet clusters [20–26], although the efficiency varied and required further optimization [27–29]. Moreover, the published protocols all require formation of cell aggregates from in suspension, a culturing condition that is different from the native niche of islets, which are supported by the exocrine ECM.

Indeed, cell-matrix interaction has been shown to play a critical role in the cell fate specification of pancreatic progenitor cells (PPs) and their commitment to endocrine progenitor cells (EPs) differentiation [21,30,31]. As a result, Matrigel-mimics have been developed to recreate the native environment of the endocrine islets to facilitate SC-β cell maturation. In particular, niches provided by collagen V (ColV) and Matrigel permitted stem cell progression into islet-like organoids with enhanced insulin and glucagon secretion in response to glucose stimulation [32]. Two poly (lactide-*co*-glycolide) (PLG) and polyethylene glycol (PEG) microporous scaffolds with 250–425 μm pore size have also been reported to provide spatial cues for hPSC-derived pancreatic progenitors, by facilitating cell assembly into clusters with enhanced β-cell function [33]. A synthetic hydrogel named Amikagel polymerized using amikacin hydrate and PEG-diglycidylether (PEGDE) was also reported to promote aggregation of hESC-derived pancreatic progenitor cells and generation of glucose-responsive islet organoids [31]. However, information regarding the exact chemical and mechanical properties required for cell-matrix interactions during the SC-β differentiation process remains lacking.

In the present study, we used Supragel, a supramolecular hydrogel formed by synthesized biotinylated peptides, for in vitro generation of SC-β clusters. The physicochemical characteristics that are specific for SC-β development have also been explored and discussed. We observed that multiple human pluripotent stem cell lines all formed cell clusters when cultured in 2D while supported by Supragel. The Supragel-cultured cell clusters were relatively uniform in size. Stem cell viability and proliferation were also better than the non-Supragel-controls. Cells cultured on Supragel also exhibited superior differentiation efficiency at all stages. The better performance of Supragel as cell culturing matrix for SC-β development is partially attributable to the effects of Supragel in determining the average size of the spontaneously formed stem cell clusters, which is achieved by tailoring the stiffness of Supragel matrix. In the present study, a stiffness of ~1.5 kPa was found to be promote uniform formation of the hPSCs into ~50–60 μm cell clusters. Besides, as peptide-composed hydrogel, the interaction between cell surface receptors (i.e. integrin receptors) and specific peptide motifs ligands (i.e. Arg-Gly-Asp, RGD) of the Supragel also contribute to the regulatory impact of Supragel on hPSCs behavior.

2. Materials and methods

2.1. Preparation of Supragel, Gel-1, Gel-2, Gel-3 and rheological tests

The preparation of Supragel hydrogel (1 wt%) was descripted by the Sifan Ai [34]. To obtain the desired concentrations of 0.25 wt%, 0.5 wt% and 0.75 wt% (2.5 mg/ml, 5 mg/ml and 7.5 mg/ml), the hydrogel was reheated and diluted with DMEM-F12 basal medium. Regarding Gel-1, a peptide derivative (15 mg) of sequence 1 was dispersed in PBS (PH 7.2–7.4) and heated by an alcohol lamp. The PH was adjusted to 7.0–7.2 using Na_2CO_3 and the solution was reheated until the powder was completely dissolved, then supplemented with PBS to a final volume of 1 ml. The hydrogel was diluted with DMEM-F12 basal medium to obtain concentrations of 5 mg/ml, 10 mg/ml and 12.5 mg/ml. Gel-2 and Gel-3 were initially prepared as gel solutions at a concentration of 8 mM (9.13 mg/ml). To maintain a constant stiffness, Gel-1 (15 mg/ml) was diluted with Gel-2 or Gel-3 and PBS to achieve a final peptide concentration of 10 mg/ml. The detailed dilution ratios were shown in Supplementary Table 1. The mechanical properties of the Supragel were measured using an Anton Paar rheometer equipped with PP25 (25 mm-diameter parallel plates) in a dynamic strain sweep with a frequency region of 0.1–10 rad s^{-1} at 1 % strain.

2.2. Human pluripotent stem cell culture and propagation

The hPSCs were maintained and passaged on Matrigel coated 6-well plates in PSCeasy® medium, as described previously [35]. Once cell confluency reached 80%–90 % after 3–4 days, the cells were harvested using 0.5 mM EDTA and resuspended into single cells with PSCeasy® supplemented with 10 μM Rho-associated protein kinase inhibitor Y-27632. The culture medium was changed daily after passaging.

2.3. hPSCs culture on Supragel or in suspension and analysis of spheroid size

For 2D Supragel culture, 1 ml of diluted hydrogel was added onto one well of a 6-well plate and then incubated overnight to form solid hydrogel surface. After harvesting hPSCs from Matrigel, they were seeded onto Supragel precoated 6-well plates or into 6-well Ultra-Low attachment plates at a density of 2×10^5 cells/cm^2 and routinely cultured in PSCeasy® medium. Morphology images of spheroids were acquired at day 1, 3, 5 and 10. The size of spheroids were measured using Image J. At least 50 spheroids in each group were randomly selected to calculate the diameter for size statistics analysis.

2.4. Cell counting kit-8 assay

The cell viability was measured via Cell Counting Kit 8 to test cell metabolism activity. hPSCs were propagated into Supragel-coated 48-well plates at a density of 5×10^5 cells/cm^2 and cultured for 5 days. On day 1, 3 and 5, the cells were treated with CCK-8 stock solution diluted with PGM1 medium at a ratio of 10:1 and incubated at 37 °C for 2 h. The absorbance of each well at 450 nm was detected by iMarkTM microplate absorbance reader.

2.5. Spheroid extraction and live-dead staining

Spheroids were cultured with Supragel for 1–10 days. To extract the

spheroids from the hydrogel, the gel was disrupted by pipetting up and down. The mixture was then transferred into 15 ml tubes and diluted with a 10-fold volume of PBS. After centrifugation at 300*g* for 5 min, the pellet was resuspended in PBS three times. The released spheroids were stained with Calcein-AM/PI staining solution for 20 min according to the manufacturer's instructions to measure cell viability. After washing three times with PBS, the spheroids were gently resuspended in a 15 ml tube and allowed to settle down by gravitation. The spheroids were then collected and transferred into glass bottom dishes for imaging using a confocal microscope. The quantification of positively stained green and red cells was performed using Image J and the area of spheroids was determined.

Cell viability was further measured using Annexin V-FITC/PI Apoptosis Detection Kit (Yeasen, 40302) to analyze the entire cell population. Briefly, spheroids were collected and incubated with Accutase (Invitrogen, 00-4555-56) to obtain a single cell suspension. After centrifugation and two washes, the cells were incubated with 100 μl of 1 × Staining Solution containing 5 μl of Annexin V-FITC and 10 μl of PI for 10 min on ice. The cells were then suspended in 400 μl of 1 × binding buffer and analyzed using a BD LSR Fortessa flow cytometer.

2.6. Stem cell differentiation

H1 cells were predominantly used throughout the study, with H7 and SF-hiPSC cells utilized to verify whether culture conditions affected the differentiation of pancreatic progenitors. For efficient differentiation of hPSCs into functional islet-like clusters (ISLCs), three conditions were employed: Matrigel-coated planar culture, Supragel-based cluster culture and suspension culture in 6-well Ultra-Low attachment plates. The ISLC differentiation protocol followed a seven-stage method derived from previously publications. Initially, hPSCs were seeded on the three conditions at densities of 2/5/10 × 10^5 cells/cm^2 with 10 μM Y27632. Cells on Matrigel reached nearly confluency while clusters formation occurred under the other two conditions after 24 h seeding. Detailed differentiation medium formulations, cytokine and small molecules information are provided in Supplementary Table 2 and Table 3. At the end of stage S3, S4 and S7, cells were collected using a 10 min TrypLE treatment for analysis. Cells on Matrigel at day 4 of S4 culture were released into single cell pellets and resuspended on filter inserts at a density of 0.5–1 × 10^6 cells per spot for further differentiation at an air-liquid interface. The frequency of media changes was also outlined in Supplementary Table 2.

2.7. Real-time quantitative PCR (RT-qPCR)

Spheroids were firstly resuspended into cell pellets using 0.5 mM EDTA and total RNA was extracted from each sample using the TRIzol. Total RNA was then reverse-transcribed into cDNA using the PrimeScriptTMRT reagent kit with gDNA Eraser and diluted to a concentration of 250 ng/μl. RT-qPCR was performed with a Bioer LineGene 9600 Plus real-time PCR detection system using Hifair® III One Step RT-qPCR SYBR Green Kit. The sequences of primers used were listed in Supplementary Table 4. The relative expression levels of target genes were normalized to the housekeeping gene TBP and the fold change was analyzed using the ΔΔCt method.

2.8. Immunofluorescence for spheroids staining

Cultured spheroids were aspirated with medium into a 15-ml tube and allowed to settle down at the bottom of the tube. They were washed once with PBS and then fixed with 4 % paraformaldehyde (PFA) for 30 min at room temperature (RT). The washing step was repeated twice and PBST solution (PBS + 0.1 % Triton X-100 + 10 % goat serum) was added for 2 h at RT to block and permeabilize the cells. The spheroids were then incubated with primary antibodies at recommended dilutions in PBST solution at 4 °C overnight. After washing three times with PBST solution, the spheroids were incubated with secondary antibodies at 1:1000 dilution for 2 h at RT. They were stained with DAPI for 15 min after three times washes and prepared for imaging. The images were captured by a Zeiss LSM 800 with Airyscan. All the antibodies used and their dilutions were listed in Supplementary Table 5.

2.9. Intracellular flow cytometry

Spheroids were incubated with Accutase for 10 min to dissociate them into a single-cell suspension and then fixed with 4 % PFA for 30 min. The digested cells were filtered through a 40 μm cell strainer and washed three times before permeabilization with PBST solution for 45 min. Next, the cells were incubated with primary antibodies overnight. After three washes, the cells were incubated with secondary antibodies for 2 h. All staining procedures were performed at 4 °C. Subsequently, the cells were washed three times in PBST solution and analyzed using a BD LSR Fortessa flow cytometer. Stem cell negative control, secondary antibody control and unstained sample control were used to gate the cell populations. For flow cytometry analysis, FlowJo V10 software was used. The antibodies also used were also listed in Supplementary Table 5.

2.10. Western blotting analysis

Spheroids were collected and dissociated into single cells using Accutase. After a single wash with cold PBS, cell pellets were resuspended in 200 μl Buffer A from the Plasma Membrane Protein Isolation and Cell Fractionation Kit (Invent, SM-005). The plasma membrane proteins were isolated according to manufacturer's instructions. Subsequently, 6 μg of membrane proteins were separated on a 10 % SDS-PAGE gel and transferred onto a PVDF membrane. The membrane was then blocked with 5 % BSA at RT for 2 h and incubated with primary antibodies at 4 °C overnight. After three times washes with PBS, the membranes were incubated with HRP-conjugated secondary antibodies. The chemiluminescence HRP substrate was used to detect the signal and the gray values of target proteins were analyzed by ImageJ which were normalized to β-actin levels.

2.11. Static glucose-stimulated insulin secretion (GSIS) and ELISA

Krebs buffer was freshly prepared according to the formulation described in Supplementary Table 6. The Krebs buffer (pH 7.3–7.4) containing 1.67 mM glucose for low glucose solutions and 16.7 mM glucose for high glucose solutions, which were both prepared and warmed to 37 °C before use. 50 hPSCs-derived islet-like clusters (ISLCs) were collected and pipetted into 24-well plate. After rinsed twice with Krebs buffer, the ISLCs were sequentially incubated with low glucose solutions, followed by low glucose solutions and then high glucose solutions. Each solution was incubated for 1 h at 37 °C and supernatants were collected for further detection. The ISLCs were then dispersed into a single-cell suspension using Accutase and cells numbers were counted to calculate the insulin content of secretion per cell. Finally, cells pellets were lysed using radioimmunoprecipitation assay (RIPA) buffer to test for remnants of insulin granules in the cells. According to manufacturer's instructions, the supernatants and cell lysates were analyzed in triplicate using a human insulin ELISA kit.

2.12. Electron microscopy

ISLCs were fixed in 2.5 % glutaraldehyde in phosphate buffer (PB: 0.1 M, pH 7.0) for more than 4 h at 4 °C. After three washes with 0.1 M PB, the samples were post-fixed with 1 % OsO_4 in phosphate buffer (0.1 M, pH7.0) for 1–2 h. Following repeated washing procedures, the samples were dehydrated using a graded series of ethanol, followed by placement in a mixture of acetone and Spurr resin to infiltrate. Samples then were embedded and ultrathin sectioned into 70 nm slices. After

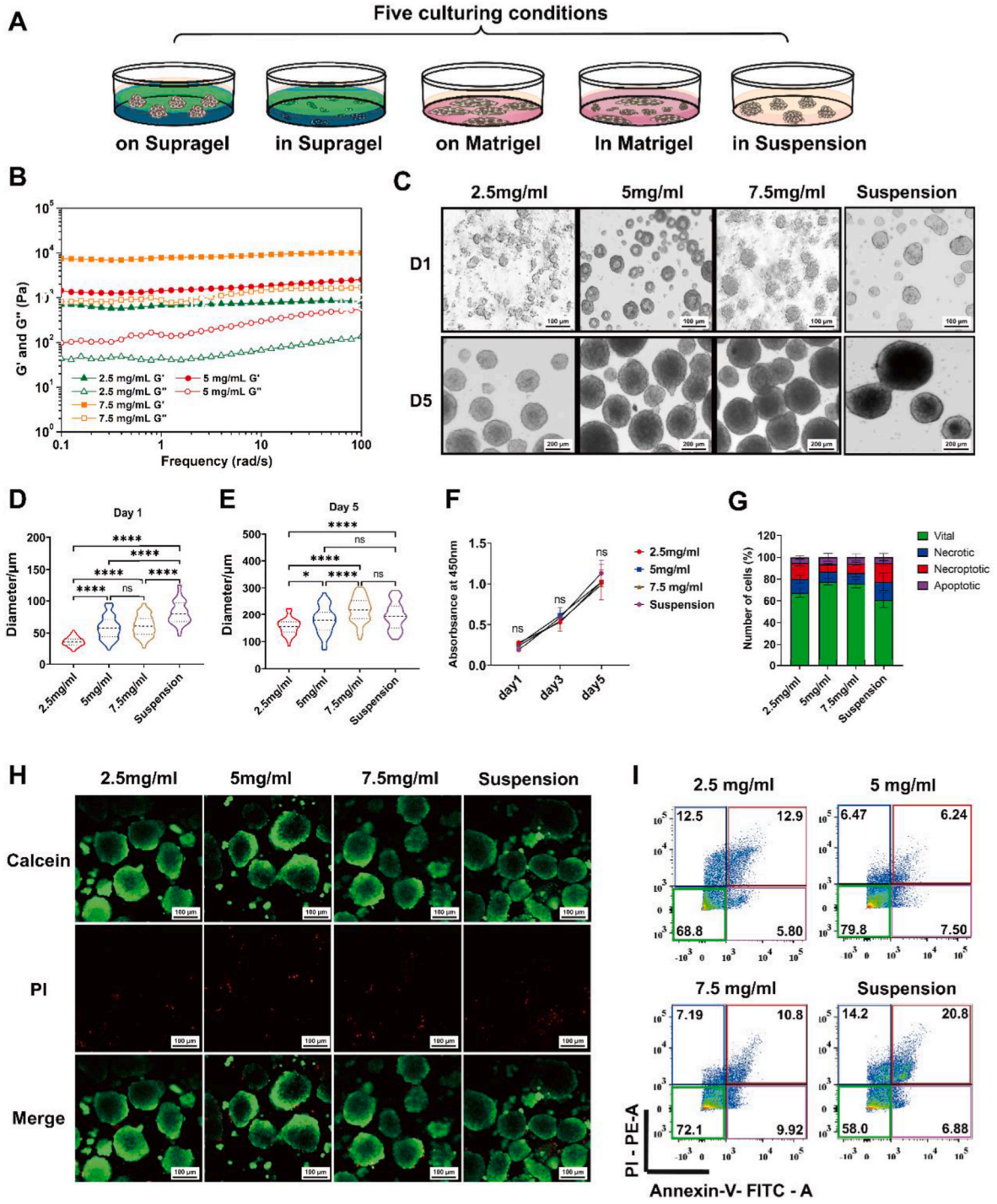

Fig. 1. The growth properties of hPSCs aggregates on Supragel or in suspension conditions. (A) The schematic diagram of five culture conditions. (B) Dynamic frequency sweep of the gel at three concentrations. (C) The morphology of H1 cell aggregates on the Supragel at three concentrations conditions or in suspension conditions. Scale bar, 100 μm (above) and 200 μm (below). (D) and (E) Quantification of the diameters of H1 cell aggregates at day 1 and day 5 on the Supragel at three concentrations conditions or in suspension conditions. Data acquired from 3 to 5 images of H1 cell aggregates with 50–100 aggregates counted. (F) Cell Counting Kit-8 assay to test proliferative ability of H1 cell aggregates at day 1, day 3 and day 5. Data are shown as means ± Standard deviations (SDs). (G) Cell viability was analyzed by flow cytometry as a percentage of live cells (Annexin V^-PI^-), necrotic cells (Annexin V^-PI^+), necroptotic cells (Annexin V^+PI^+) and apoptotic cells (Annexin V^+PI^-) of the total cells. n = 4. (H) Aggregates of H1 cell grown on the Supragel or in suspension at day 5 were stained with dyes for live (Calcein, green) and dead (PI, red) cells. Scale bar, 100 μm. (I) Representative flow cytometry plot of cell viability and the cell proportions of live, necrotic, necroptotic and apoptotic cells in H1 dispersed cells at day 5. Data are shown as means ± SDs. *: $p < 0.05$, **: $p < 0.01$ and****: $p < 0.001$, ns: no significance.

staining with uranyl acetate and alkaline lead citrate, the grids were observed with a Talos F200C transmission electron microscope.

3. Results and discussion

3.1. Supragel promotes hPSCs aggregation into cell clusters

In order to choose a suitable culturing condition, H1 cells were cultured by mixing within the Supragel (In Supragel), seeding on the Supragel matrix (On Supragel), in Matrigel, on Matrigel or in suspension, as illustrated in Fig. 1A. Cells from the Matrigel group displayed typical flattened and stretched monolayered colonies (Fig. S1A, on Matrigel). In contrast, for cells seeded on top of the Supragel matrix, spontaneous formation of spherical clusters was observed. These cells exhibited relatively uniformed cell spheres with smooth borders (Fig. S1A, on Supragel) instead of the random rhomboid cell masses

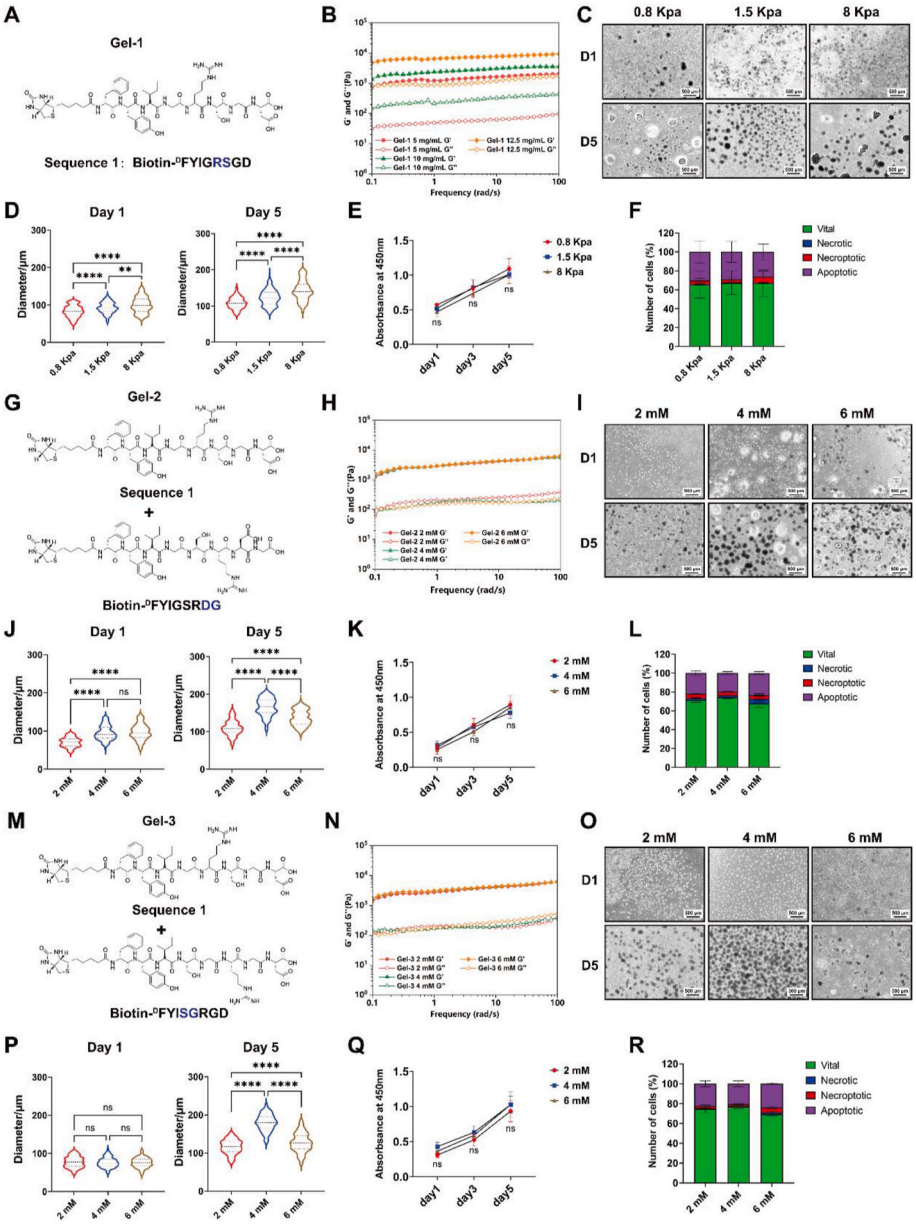

Fig. 2. The growth properties of hPSCs aggregates on Gel-1, Gel-2 and Gel-3 conditions. (A) Chemical structure of the Biotin-^{D}FYIGRSGD gelator. (B) Dynamic frequency sweep of the gel at three concentrations (LS, low stiffness; MS, medium stiffness; HS, High stiffness). (C) The morphology of H1 cell aggregates on the Gel-1 at three stiffness conditions. Scale bar, 500 μm. (D) Quantification of the diameters of H1 cell aggregates at day 1 and day 5 on the Gel-1 at three stiffness conditions. Data acquired from 3 to 5 images of H1 cell aggregates with 50–100 aggregates counted. (E) Cell Counting Kit-8 assay to test proliferative ability of H1 cell aggregates at day 1, day 3 and day 5. Data are shown as means ± Standard deviations (SDs). (F) Cell viability was analyzed by flow cytometry as a percentage of live cells (Annexin V^{-}PI^{-}), necrotic cells (Annexin V^{-}PI^{+}), necroptotic cells (Annexin V^{+}PI^{+}) and apoptotic cells (Annexin V^{+}PI^{-}) of the total cells. n = 4. (G) and (M) Chemical structure of the Biotin-^{D}FYIGSRDG and Biotin-^{D}FYISGRGD gelator, respectively. (H) and (N) Dynamic frequency sweep of the gel with a relatively constant stiffness when three different concentrations of Biotin-^{D}FYIGSRDG and Biotin-^{D}FYISGRGD peptides were added, respectively (LC, low concentration; MS, medium concentration; HS, High concentration). (I) and (O) The morphology of H1 cell aggregates on the Gel-2 and Gel-3 at three concentration conditions, respectively. Scale bar, 500 μm. (J) and (P) Quantification of the diameters of H1 cell aggregates at day 1 and day 5 on the Gel-2 and Gel-3 at three concentration conditions, respectively. Data acquired from 3 to 5 images of H1 cell aggregates with 50–100 aggregates counted. (K) and (Q) Cell Counting Kit-8 assay to test proliferative ability of H1 cell aggregates at day 1, day 3 and day 5. Data are shown as means ± Standard deviations (SDs). (L) and (R) Cell viability was analyzed by flow cytometry. n = 4. **: $p < 0.01$ and****: $p < 0.001$, ns: no significance.

from the 3D Supragel group (Fig. S1A, In Supragel). Cells cultured in Matrigel exhibited mixed spheroids and colony phenotypes rather than uniform hPSC aggregation into cell clusters, regardless of the Matrigel volumes and initial cell seeding densities (Fig. S1C, In Matrigel). As a result, the "On Supragel" culture condition was selected as a more suitable cluster formation for the hPSCs in the present study and used for subsequent investigation.

As previously reported, the Supragel was self-assembled by a series of peptide sequences, containing the fibronectin-derived three-amino-acid peptide Arg-Gly-Asp (RGD) and laminin-derived pentapeptide Tyr-Ile-Gly-Ser-Arg (YIGSR) [34]. By varying the peptide concentration, it could be tailored into variations with different biophysical and biochemical properties. Given that these properties of synthetic matrices have been shown to influence stem cell differentiation and function [36], we first attempted to identified the suitable physicochemical characteristics of the Supragel for 2D hPSCs culturing.

Based on previous studies [34], three Supragel concentration (2.5 mg/ml, 5 mg/ml and 7.5 mg/ml) were selected, each giving rise to a different stiffness. Results from the rheological test indicated that the storage modulus increased with the Supragel peptide concentration (Fig. 1B). Although the H1 cells formed cell clusters regardless of Supragel stiffness, the degree of stiffness appeared to affect the size of H1 cell clusters (Fig. 1B and C). On day 1 of cell culturing, the average diameters of cell clusters were ~36, 58, and 62 μm for 2.5, 5 and 7.5 mg/ml Suprage-based culturing conditions, respectively (Fig. 1D). For all conditions, the size of cell clusters increased with time due to cell expansion (Fig. 1E and F) and at day 5, the average diameters of cell clusters were ~150, ~180 and ~220 μm for 2.5, 5 and 7.5 mg/ml Supragel, respectively (Fig. 1E). In comparison, cells maintained in suspension formed significantly larger spherical clusters by day 1, with diameters between ~80 and 100 μm, and increased to ~250–280 μm by day 5 (Fig. 1C–F). The H1 clusters cultured in all conditions showed viability above ~80 %, although for H1 cell cultured with the 2.5 and 5 mg/ml Supragel, moderate yet statistically significant improvement of cell viability was observed, implicating better cell viability of the comparatively smaller cell clusters (Fig. 1H and S1B). We further evaluated cell death (early and late apoptosis, as well as necrosis) by flow cytometry using Annexin V-FITC/PI staining. Although there was moderate overestimation of cell viability by staining per se, the viability of H1 clusters was above ~70 % in all Supragel cultured conditions (Fig. 1G–I and Table S7). When H1 cells were cultured for a prolonged period of 10 days on Supragel, although there was no significant difference in cell expansion among the 2.5, 5 and 7.5 mg/ml Supragel groups, cell viability observed from the 5 mg/ml group (~80 % by day 10) was significantly higher (Figs. S1E–J). In contrast, cell clusters maintained in suspension were only half viable, showing only ~50 % cell viability, significantly lower than all Supragel groups (Figs. S1H and S1I). Similar results were also observed using the H7 and hiPSCs (derived from renal epithelial cells) cell lines (Figs. S2–S3).

To further investigate the exact mechanisms regarding Supragel stiffness, we synthesized and prepared a Biotin-^{D}FYIGRSGD hydrogel (Sequence 1, Gel-1) as a mechanical control (Fig. 2A). Results from the rheological test indicated that although Gel-1 had two shuffled peptide sequences, its storage modulus was similar to Supragel's stiffness and the stiffness also increased with the peptide concentration (Fig. 2B). The degree of stiffness slightly affected the size of H1 cell clusters (Fig. 2B–D), with the average diameters of H1 clusters maintained around ~83–143 μm during 5 days of culturing, which were significantly smaller than those in the Supragel groups (H1 clusters were larger than 150 μm at day 5). Flow cytometry analysis using Annexin V-FITC/PI staining also showed that there were ~60 % live cells and ~30 % apoptosis cells in all Gel-1 cultured conditions (Fig. 2E and F and Table S7).

To explore how specific peptide sequences affect the Supragel-cell interactions at cell adhesion sites, we designed and synthesized Biotin-^{D}FYIGSRDG (Sequence 2) and Biotin-^{D}FYISGRGD (Sequence 3), each differing by only one shuffled peptide sequence (Fig. 2G and M). We then prepared Gel-2 and Gel-3 with relatively stable stiffness by supplementing Gel-1 with Sequence 2 and Sequence 3 at final concentrations of 2 mM, 4 mM and 6 mM, respectively (Fig. 2H and N). On day 1 of cell culturing, the average diameters of cell clusters increased with the peptide concentration in Gel-2 conditions, while clusters in Gel-3 conditions remained similar across all concentration (~75 μm) (Fig. 2J and P). Only at a concentration of 4 mM, the size of cell clusters increased to ~165 μm and 180 μm in Gel-2 and Gel-3 culturing conditions, respectively, by day 5 (Fig. 2J and P). Cell death analysis showed the best cell viabilities in Gel-2 and Gel-3 culturing conditions with a peptide concentration of 4 mM, similar to the peptide concentration in the 5 mg/ml Supragel group (Fig. 2L, R and Table S7). These results suggests that the mechanical stiffness of Supragel facilitates hPSC cluster formation and the RGD and YIGSR peptides may promote hPSC growth.

Matrigel was initially applied in the feeder-free hESC culture system to maintain undifferentiated cells for up to 130 population doublings. Typically, hPSC maintain a spindle-like morphology on Matrigel the day after seeding and grow as monolayer colonies with a doubling time of 31–33 h [37]. To support the growth of undifferentiated hPSC, Matrigel serves as a complex matrix containing multiple ligands that bind to the integrin receptors α5, α6, αv, β1 and β5 of hPSC. These interaction are crucial for their expansion and maintenance of pluripotency [8]. However, although the presence of peptides RGD and YIGSR in Supragel, which facilitate ubiquitous binding to cell surface integrin receptors, we found that hPSCs aggregates into clusters in our Supragel-based culture system. Ordinarily, cells only formed aggregates in the absence of typical cell binding sites on 2D hydrogel, which was similar to the environment lack of cell-ECM interaction observed in low attachment plates (in suspension) [38]. There may be lack of specific receptors to maintain the stretched morphology of hPSCs clusters cultured on Supragel, a detailed investigation of the specific types of integrin receptors in hPSCs clusters is needed. The mechanical stiffness of the matrix may also influence hPSCs cell cluster formation. Improvement in terms of cell viability and uniform cluster formation was observed in softer Supragel (with initial stiffness of 0.8 and ~1.5 kPa). Further investigation into the effect of mechanical stiffness on the maintenance of pluripotency or spontaneous differentiation of hPSC clusters under the condition of Supragel or suspension should also be considered.

3.2. *Supragel promotes integrin receptor expression of the hPSCs cluster to facilitate definitive endoderm differentiation*

Previous reports have shown that the stiffer substrate could switch the fate of mesenchymal stem cells (MSC) into osteogenic lineage while softer substrate tended to promote fat or neuronal differentiation [39,40]. Considering that the pluripotential cells in their native embryonic state can spontaneously differentiate into various cell types [37], we further examine the effect of Supragel stiffness on the maintenance of pluripotency or differentiation capability of hPSCs. This includes assessing pluripotency markers or differentiation tendencies toward the three germ layers markers.

As shown in Fig. 3A and B, decreased expression levels of *NANOG* and *OCT4*, two essential transcription factors for the maintenance of the pluripotent stem cell phenotype, were observed in cells cultured on Supragel or in Suspension when compared to the Matrigel group. These two gene expression levels were also decreased in the mechanical control groups (Gel-1 culture condition) and the peptide sequences control groups (Gel-2 and Gel-3 culture conditions) (Fig. S5A). This suggests that hPSC clusters under these conditions may shift towards differentiation rather than maintenance of pluripotency. However, the Supragel group exhibited comparatively better pluripotency maintenance than those in suspension condition (Fig. 3A and B). Moreover, considering the tendency of hPSCs to form cell spheres spontaneously when seeded on top of Supragel, it may indicate more committed differentiation of these cells, which could be important for specific organoid generation.

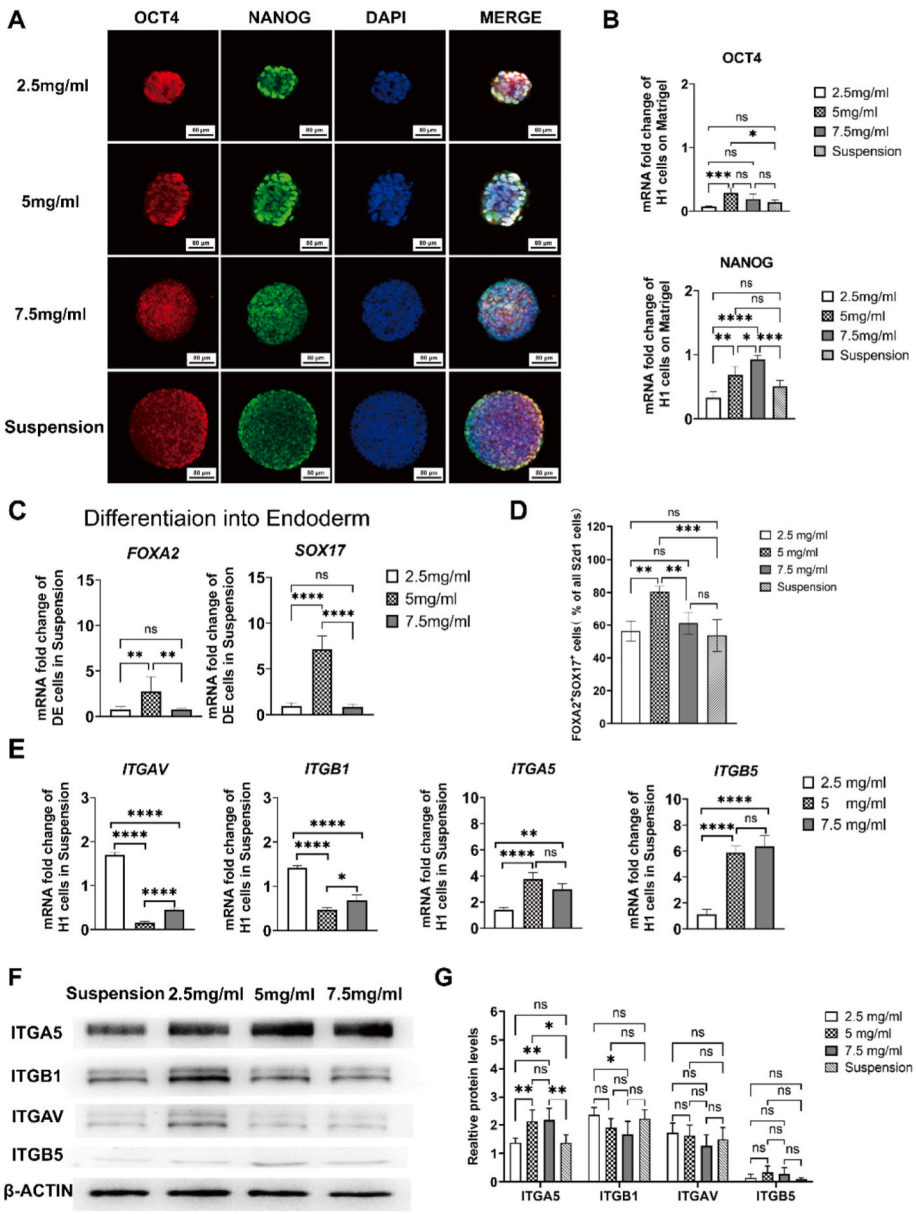

Fig. 3. hPSCs Aggregates on Supragel Promotes Definitive Endoderm Differentiation via Elevated Integrin Receptor Expression Compared to those in Suspension. (A) Fluorescent images showed the expression of pluripotency markers NANOG and OCT4 in cell nucleus at day 5 on the Supragel or in suspension. Scale bars, 80 μm. (B) The pluripotency-related genes of *NANOG* and *OCT4* expression levels determined by RT-qPCR. The results from the H1 cells grown on the Matrigel as a reference to calculate the fold changes. (C) Expression levels of definitive endoderm-related genes *FOXA2* and *SOX17* on Supragel at three different concentrations in direct differentiation trial, as determined by RT-qPCR. The results compared to H1 cells differentiation in suspension. (D) Representative flow cytometry statistical analysis of the FOXA2^{+} SOX17^{+} cell proportions in DE dispersed cells at day 5 under four various conditions. (E) Expression levels of adhesion-related genes, including integrin αv (*ITGAV*), integrin β1 (*ITGB1*), integrin α5 (*ITGA5*), and integrin β5 (*ITGB5*) on Supragel at three different concentrations, as determined by RT-qPCR. The results from the H1 cells grown in suspension as a reference to calculate the fold changes. (F) Western blotting analysis of clusters on Supragel at three different concentrations and in suspension, revealing the expression of adhesion-related membrane proteins ITGAV, ITGB1, ITGA5 and ITGB5, β-ACTIN used as a loading control. (G) Graphs showing the quantitative analysis of the ITGAV, ITGB1, ITGA5 and ITGB5 proteins, compared with the amount of β-ACTIN protein. Data are shown as means ± SDs. ****: $p < 0.001$, ***: $p < 0.005$, **: $p < 0.01$ and *: $p < 0.05$, ns: no significance. For above all genes $n = 3$ biological replicates, $n = 3$ technical replicates per group.

Interestingly, the expression levels of genes related to ectoderm and mesoderm were significantly lower in the Supragel group (Figs. S4A–C, fold changes were normalized to value of the suspension group). It was notable that the expression levels of *SOX17* and *FOXA2*, markers for the DE, were significant higher in the 5 mg/ml and 7.5 mg/ml Supragel groups (Figs. S4C–E). We further verified the impact of Supragel on the DE differentiation with the combination of CHIR-99021 and Activin A. The qPCR results confirmed upregulation of *SOX17* and *FOXA2* in all Supragel groups, with the highest expression levels observed in the 5 mg/ml group (Fig. 3C). Flow cytometry results shown that the efficiency of SOX17^{+}FOXA2^{+} DE induction was approximately 80 % in H1 cell clusters from the 5 mg/ml group (Fig. 3D and S4F), which significantly higher than clusters cultured in other three groups.

To further investigate the exact mechanisms of Supragel stiffness and Supragel-cell interactions in DE differentiation, we performed differentiation under similar stiffness using Gel-1 and under different peptide concentrations using Gel-2 and Gel-3 cultured conditions. The qPCR results showed increased expression levels of *SOX17* and *FOXA2* in all

gel-cultured conditions (Fig. S5B). The fold changes were significantly higher with 5 mM RGD peptide (Gel-3), while moderate changes were observed with 2 mM YIGSR peptide (Gel-2) (Fig. S5B). However, DE induction efficiencies were ~30 %, ~40 % and ~50 % in Gel-1, Gel-2 and Gel-3 groups respectively, which were significantly lower than those in all Supragel groups ((Fig. S5C). This suggests that the Supragel matrix combining YIGSR and RGD peptides with a stiffness around 1.5 kPa may facilitate hPSC cluster differentiation toward DE.

In addition to the mechanical effect of Supragel, differentiation of the Supragel-cultured hPSCs could also be influenced by the interactions between peptides and cells [41,42]. Indeed, the Supragel is chemically composed of amino acid sequences containing the RGD motifs, which are molecular ligands to all integrin receptors [43]. The integrin receptors are a set of unique cell surface receptors, via which effects on stem cell survival, spreading and self-renewal has been demonstrated [42–45]. In general, integrin receptors serve as bidirectional cell signaling depots. They not only respond to extracellular changes to regulate cellular processes such as proliferation and gene expression, but also relay internal cellular signals to the cell membrane for modulation of cell behaviors including cell spreading, migration and so on [46]. The integrin receptors often contain an α and a β subunit. In mammals, most integrin α-subunits can only form one heterodimer with one β-partner, while α4 and αv can interact with more than one β-partner, including α4β1, α4β7, αvβ1, αvβ3 and αvβ5. Additionally, the β1 subunit can form heterodimeric complexes with 12 α-subunits, whereas β4, β5, β6, and β8 only interact with the αv subunit [47]. Previous study has reported that Supragel containing the combination amino sequences of YIGSR and RGD enhanced the paracrine function of MSC via integrin α2β1 and the PI3K/AKT signaling pathway in acute kidney injury [48]. Here, we expect the Supragel, by containing the RGD and YIGSR motifs, may also affect the hPSCs differentiation via the adhesion motifs of integrin receptors.

We observed significantly higher expression of integrin α5 and β5 in the 5 mg/ml and 7.5 mg/ml Supragel groups while integrin αv and β1 were highly expressed in the 2.5 mg/ml Supragel group (Fig. 3E). Modest increase of integrin α2 and reduction of integrin α6 were also observed in the Supragel groups (Fig. S4G). Moreover, the qPCR results were further confirmed by western blotting data (Fig. 3F and G), both of which suggest a distinct relationship between cell-matrix feedback in the formation of cell clusters in Supragel-based and suspension culture conditions. The expressing levels of integrin receptors of αv, β1, α5 and β5 increased with stiffness in Gel-1 culture condition (Fig. S5D). There were no differences in the expression levels of integrin αv and β1 when clusters cultured with Gel-2, while integrin α5 and β5 were significantly higher in the 2 mM YIGSR group (Fig. S5E). The RGD peptide seems to have a greater effect on the expression levels of integrin αv, α5 and β5 in Gel-3 culture condition, as the expression patterns of these genes were similar to those in Supragel groups (Fig. S5F). Thus, we hypothesize that Supragel with low stiffness may interact with hPSCs through integrin αvβ1 binding, while integrin α5β1, αvβ5 and α2β1 may participate in the interaction between high stiffness of Supragel and hPSCs. These interactions may play a role in directing hPSCs differentiation, as previous studies have reported the regulation of endoderm differentiation through the expression of integrin α5, integrin αv and integrin β5. Considering the multifaceted roles of integrin receptors in a variety of cellular behaviors [46], further investigation regarding the exact cell-Supragel interaction via the RGD-integrin receptors is required.

3.3. *Optimizing culture conditions for efficient generation of pancreatic progenitor cells clusters on Supragel*

Given the morphological resemblance between the Supragel-cultured hPSCs clusters and the pancreatic islets, as well as the preferred differentiation of the Supragel hPSCs clusters toward endoderm origin, we then investigated the potential of hPSCs toward the pancreatic progenitor cells, which directly determines efficiency of obtaining glucose-responsive and monohormonal insulin-producing cells [21,25,28]. The Supragel-cultured H1 cell clusters were induced into pancreatic progenitor 1 and 2 cells (PP1 and PP2) by following protocol published by Hogrebe et al. (Protocol P), a standard method for β-cell differentiation on Matrigel [28]. Although the protocol P was amenable for differentiating PP1 cells, the exact cell density must be optimized for each cell line at the beginning of the differentiation [28]. We chose the 5 mg/ml group to induce H1 cell clusters into PP1clusters under three initial seeding densities (2×10^5 cells/cm^2 indicated as low SD, 5×10^5 cells/cm^2 indicated as medium SD and 1×10^6 cells/cm^2 indicated as high SD) to optimize the Supragel-based differentiation culture system (indicated as cluster). In parallel, cells were also cultured in suspension (indicated as suspension) and on Matrigel (indicated as planar) with the same three seeding density (Fig. 4A).

Regarding morphological characteristics of cells that were maintained in different conditions, for the Matrigel group, the cell reached >95 % confluency at the initial stage of differentiation when seeded at medium SD and maintained a confluency layer without any gaps throughout 1–4 stages. At the beginning of stage 3, the cell layers grew thicker with an epithelial-like morphology and retained a crowded appearance (Fig. 4B and S6A). The cells seeded on Matrigel with low SD detached from the cell layer at early stage 2, while those seeded with high SD remained jammed without morphology changes (Fig. S6B). Cells cultured on Supragel or in suspension both exhibited a rounded morphology without any outer layers at the periphery of the aggregates, which became larger and darker over time (Fig. 4C and S4A). The average size of the cell clusters also increased with increased seeding densities. For the Supragel group, the clusters were comparatively smaller sizes than those in the suspension groups, independent of the initial seeding densities (Figs. S6C and S6D).

We found that the efficiency of PDX1$^+$ PP1 induction was significantly higher in H1 cell clusters from the 5 mg/ml group at any initial seeding density, giving an induction efficiency of approximately 80 % at both low and medium SD. In contrast, for suspension and Matrigel conditions, the induction efficiency only reached ~80 % at low SD (for suspension) and medium SD (for Matrigel) (Fig. 4B–D and S7A). As a result, achieving high induction efficiency of PP1 cell generation (~80 %) on Supragel appeared to be less dependent on the initial cell seeding density when compared to both the Matrigel and the suspension conditions (Fig. 4F). High SD in all culturing conditions resulted in less sufficient (<60 %) PP1 differentiation and was therefore excluded.

Regarding the induction efficiency of PDX1$^+$/NKX6.1$^+$ PP2 cells, Supragel-cultured clusters gave an induction efficiency of ~34.6 % and ~30 %, with low and medium SD, respectively. For cells maintained in suspension, only ~2.92 % and ~3 % induction efficiency was observed, similar to those differentiated on Matrigel, showing ~4 % and ~24.7 % efficiency with low and medium SD, respectively (Fig. 4E–G and S7B). The significantly reduced induction efficiency from cells maintained in suspension could be in part due to larger cell clusters (up to ~550 μm in diameter) (Fig. 4H). The H7 and hiPSC cell lines exhibited similar tendency regarding induction efficiencies for the PDX1$^+$ PP1 and PDX1$^+$/NKX6.1$^+$ PP2, with high efficiency observed from the Supragel group (Fig. S8). It is worth noting that for the H7 cells, only the Supragel-cultured cell clusters differentiated into PP1 and PP2 cells (Figs. S8C–F). The Matrigel-cultured non-clustered H7 cells failed to differentiation (Figs. S8C and S8D).

We further validate the effects of Supragel stiffness on pancreatic progenitors (PP) differentiation. The cell clusters were obtained after 8 days (PP1) and 12 days (PP2) of induction on Supragel with the stiffness of 0.8 kPa (2.5 mg/ml), 1.5 kPa (5 mg/ml) and 8 kPa (7.5 mg/ml) (Fig. 5A). Only the PP1 and PP2 clusters from the 5 mg/ml Supragel group exhibited uniformed cluster formation, giving an average diameter of ~200 μm. In contrast, cell cultured with either 2.5 mg/ml or 7.5 mg/ml Supragel groups showed significant variation in size, with average diameters ranging from ~90 μm to ~350 μm in diameter (Fig. 5B and C). Flow cytometry and immunofluorescence results

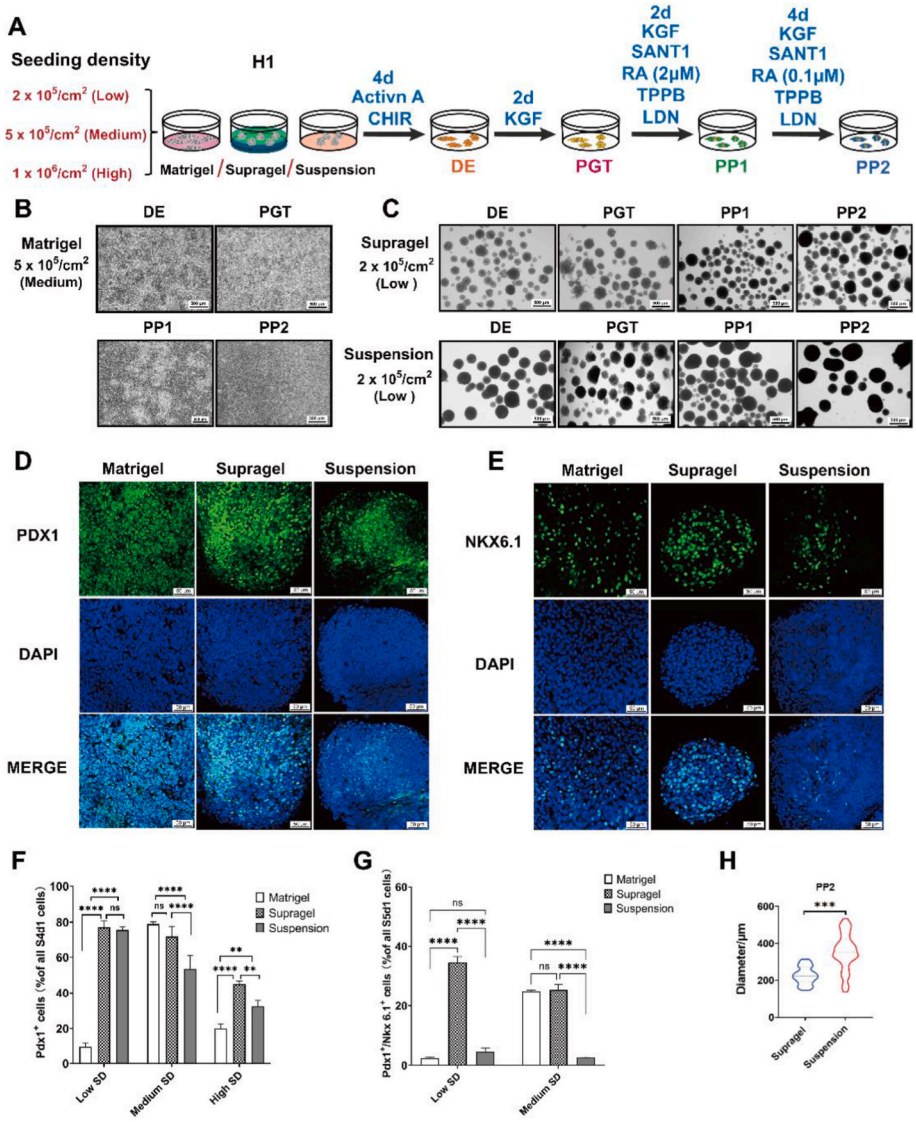

Fig. 4. Optimizing initial seeding density and culture method for efficient generation of pancreatic progenitor cells at Stage 3 and Stage 4. (A) Schematic diagram illustrating the differentiation of H1 cell aggregates into PP1 and PP2, depicting the changes in cell fate under three various conditions (Planar culture on Matrigel, cluster culture on Supragel and suspension culture) with three different initial seeding densities. (B) and (C) Morphology of DE, PGT, PP1 and PP2 cells at three culture conditions with optimized seeding cell density. Scale bar, 500 μm. (D) and (E) Immunofluorescence staining of PDX1 in PP1 cells and NKX6.1 in PP2 cells under three various conditions corresponding to the medium SD on Matrigel and the low SD on the gel and in suspension culture conditions, respectively. Scale bar, 50 μm. (F) and (G) Representative flow cytometry statistical analysis of the PDX1$^+$cell proportions in PP1 dispersed cells at day 8 and the PDX1$^+$NKX6.1$^+$cell proportions in PP2 dispersed cells at day 12 under three various conditions with three initial seeding density. (H) Quantification of the diameters of PP2 cell aggregates at day 12 on Supragel and in suspension conditions. Data acquired from 3 to 5 images of PP2 cell aggregates with 50–100 aggregates counted. Data are shown as means ± SDs. **: $p < 0.01$, ***: $p < 0.005$ and ****: $p < 0.001$, ns: no significance.

revealed that approximately 80 % of H1 cell clusters on the 5 mg/ml group were successfully induced into PDX1$^+$ PP1 cells. In contrast, the induction efficiency for PDX1$^+$ PP1 cells was only ~40 % on 2.5 mg/ml group and ~50 % on 7.5 mg/ml group (Fig. 5D and E). At 12 days of induction, significantly higher efficiency of PDX1$^+$/NKX6.1$^+$ PP2 cells generation was also observed in the 5 mg/ml group compared to the other two groups (Fig. 5F and G).

It has also been reported that during differentiation, certain segments of the integrin receptors as well as the cellular adhesive properties would change, thus increasing the chances of aggregation formation of the hESC-derived pancreatic progenitors (hESC-PPs) [31]. Since the Supragel contains peptide sequences that are ligands of the integrin receptor, we also explored whether Supragel affected the induction efficiency of PP1 and PP2 by measuring the expression levels of integrin receptor mRNAs at the end of PP2 induction. Interestingly though, no significant changes in integrin receptor gene expression were observed, suggesting a lesser influence of Supragel on integrin receptors activities in these later differentiation stages (Fig. S7C).

In addition, it has also been shown that one of the Supragel component, laminin-derived peptide YIGSR, was able to enhance the expression of E-cadherin, which has been reported to correlate with insulin secretion [49] and promote 3D-generation of the pancreatic ductal epithelial cells [50–52]. Activation of E-cadherin by PDX1 binding has also been shown in pancreatic cell fate specification and organogenesis in vivo.

In the present study, we have subsequent observed increased E-cadherin mRNA and protein expressions of Supragel-cultured clusters at the end of PP2 induction from the 5 mg/ml Supragel group (Fig. 5H and I), suggesting a potential involvement of E-cadherin in hPSCs differentiation through facilitating cell-to-cell adhesion at later stages of PP

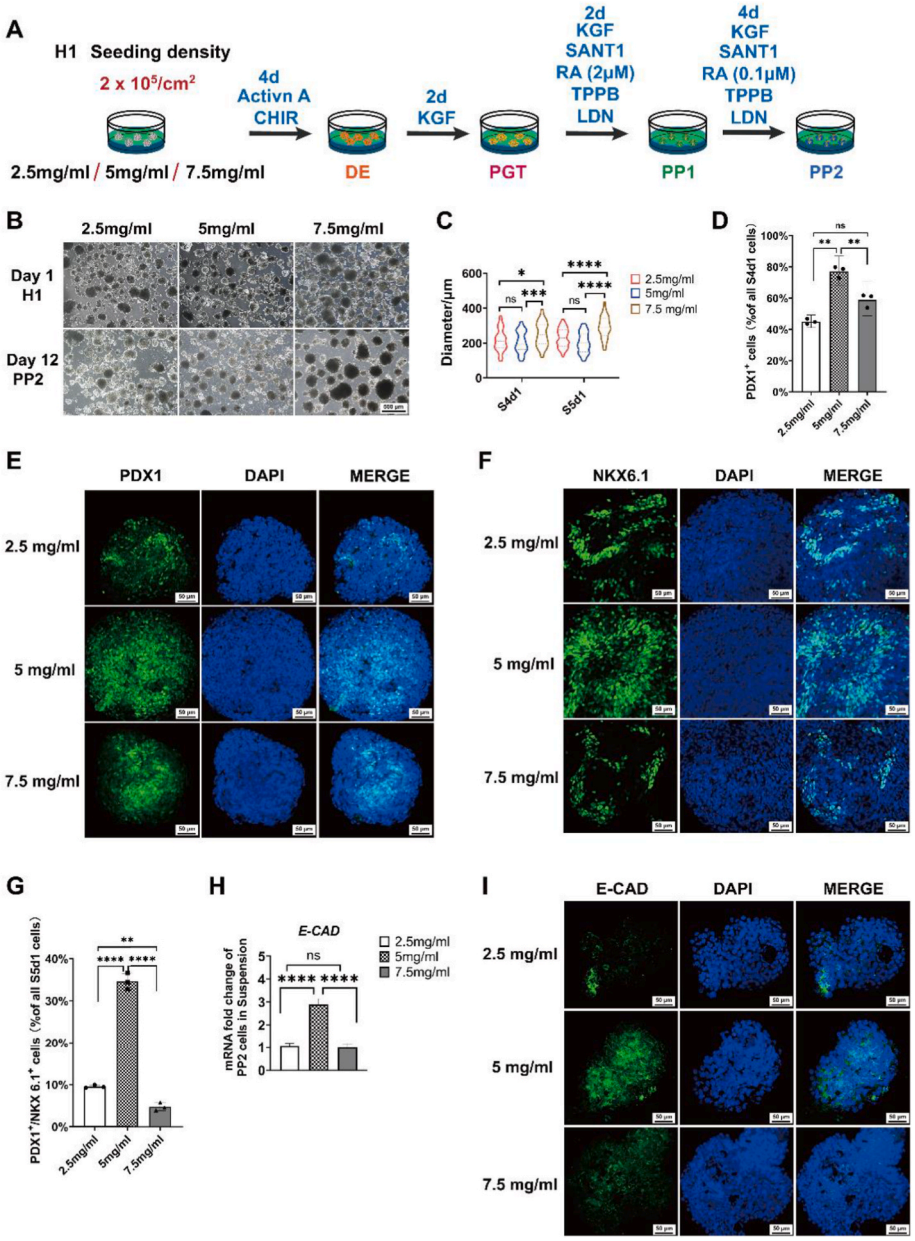

Fig. 5. Optimizing gel concentrations for efficient generation of pancreatic progenitor cells at stage 3 and 4. (A) Schematic diagram of H1 cell aggregates differentiation into PP2, depicting the changes in cell fate on Supragel under three gel concentration conditions with the same initial seeding density. (B) H1 cell aggregates morphology on Supragel at concentration of 2.5 mg/ml, 5 mg/ml and 7.5 mg/ml at day 1 and PP2 cell aggregates on day 12. Scale bar, 500 μm. (C) Quantification of H1 cell aggregates diameters at day 8 and day 12 on Supragel at concentration of 2.5 mg/ml, 5 mg/ml and 7.5 mg/ml. Data acquired from 3 to 5 images of PP1 and PP2 cell aggregates with 50–100 aggregates counted. (D) Flow cytometry analysis of $Pdx1^+$ cell proportions in PP1 under three gel concentration conditions. (E) and (F) Immunofluorescence staining of PDX1 and NKX6.1 in PP1 and PP2 cell aggregates respectively under three gel concentration conditions. Scale bar, 50 μm. (G) Flow cytometry analysis of $Pdx1^+Nkx6.1^+$ cell proportions in PP2 aggregates under three gel concentration conditions. (H) and (I) RT-qPCR analysis and immunofluorescence staining of E-cadherin in PP2 cell aggregates under three gel concentration conditions, respectively. Scale bar, 50 μm. Data are shown as means ± SDs. *: $p < 0.05$, **: $p < 0.01$, ***: $p < 0.005$ and ****: $p < 0.001$, ns: no significance. For above all genes n = 3 biological replicates, n = 3 technical replicates per group.

differentiation. Thus, we propose that the Supragel cell culture system facilitates spontaneous cell formation into uniformed clusters by providing appropriate stiffness and adhesion motifs, and therefore improves differentiation efficiency of PP1 and PP2 with less dependence on the initial cell seeding density.

Various research groups have reported efficient hPSCs differentiation into pancreatic progenitors and β-cells in 2D adherent and 3D suspension-based culture [20,23,24,26,30]. However, the cell initial seeding density, induction recipe and the origin of selected cell lines were less well examined in relation to their respective induction efficiency [53,54]. In the current study, we confirmed that in 2D planar condition, the induction efficiency of pancreatic progenitors depend both on the initial seeding density and choice of cell lines. However, the use of Supragel-based culture system was more tolerant for pancreatic progenitor differentiation by being less dependent on these factors.

The superior effects of Supragel on promoting hPSC differentiation were partly attributed to the spontaneous formation of cell clusters into appropriate size (200 μm in diameter at the end of stage 4). It was reported that cell aggregates exceeding ~400–~500 μm in diameter could hinder the passive transportation of nutrients, gas exchange as well as

growth factors and other molecular cues into the center of cluster [55,56]. As a result, although efficient PDX1$^+$ cells were obtained at the end of PP1induction in the suspension group, the considerable lager clusters would hinder the transportation of differentiation factors, leading to insufficient activation of NKX6.1 for the subsequent PP2 differentiation. Earlier reports have shown that constant agitation or spinning in bioreactors were applied to facilitate diffusion of nutrient supply to the center of cell aggregates during pancreatic progenitor cells differentiation [20,23]. With our Supragel-based culture system though, the culturing condition for hPSC differentiation are easily applicable.

However, it is worth noting that with the use Supragel, the physiochemical properties still require fine tuning for the requirement of pancreatic progenitor differentiation, as we did observe insufficient differentiation of PP1 and PP2 using 2.5 mg/ml and 7.5 mg/ml Supragel. One possible factor here may be the difference in the size of PP1 and PP2 clusters, although the PP1 and PP2 clusters from both the 2.5 and 7.5 mg/ml Supragel group were not as uniformed as from the 5 mg/ml group, they are still smaller (below ~400 μm) and smoother than those in suspension.

Given the above reasons, the more essential factor that participated in Supragel-facilitated pancreatic progenitor differentiation would be cell surface adhesion. By providing a combination of stiffness level and sites for cell adhesion, the Supragel, 5 mg/ml in specific, promoted spontaneous hPSCs aggregation into uniformed cell clusters (~58 μm).

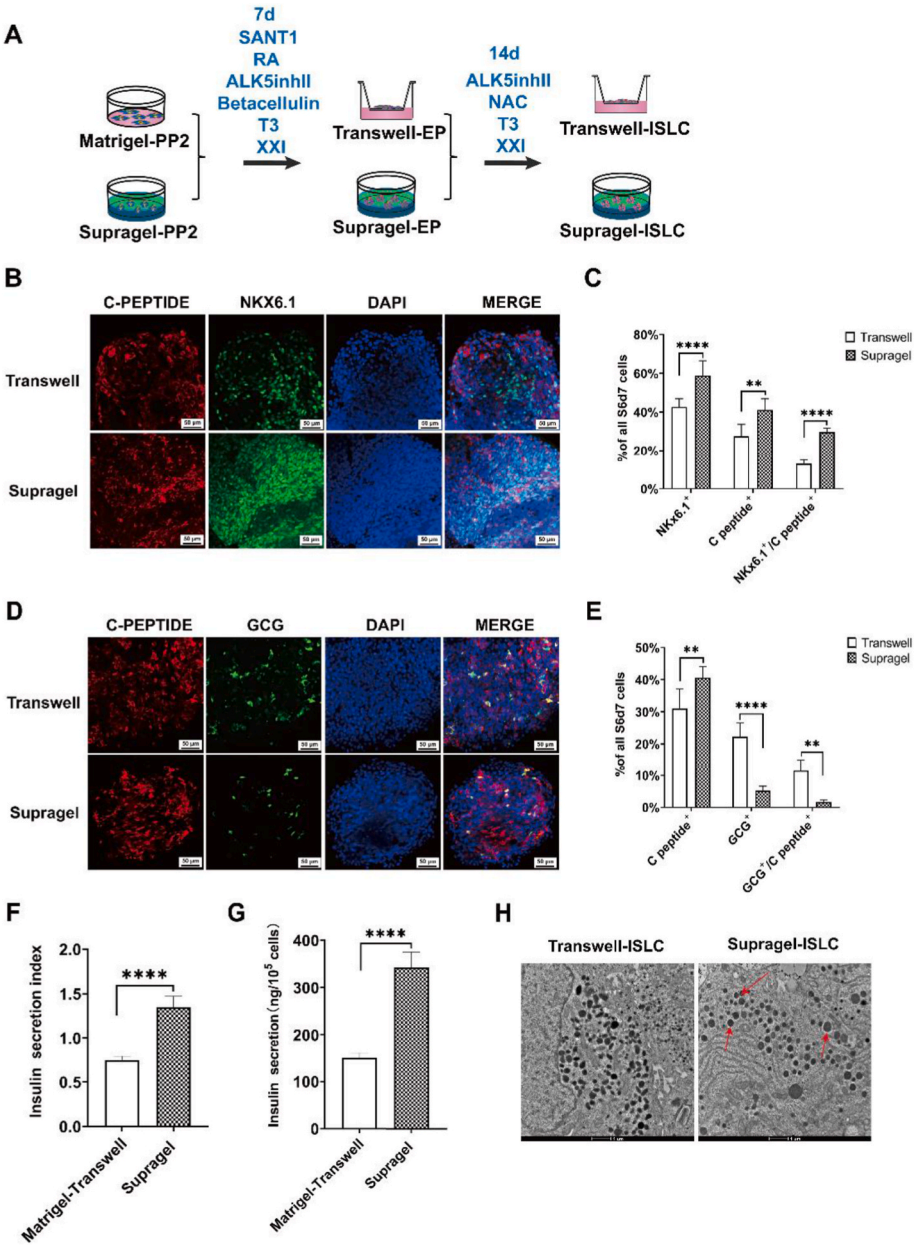

Fig. 6. Generation of glucose-responsive islet-like clusters on Supragel compared to on Transwell culture. (A) Schematic diagram illustrating the differentiation of PP2 cell aggregates into islet-like cell aggregates (ISLC), depicting the changes in cell fate on Transwell and on Supragel. (B) Immunofluorescence staining of C-PEPTIDE and NKX6.1 in ISLC on Transwell and Supragel conditions. Scale bar, 50 μm. (C) Cell proportions of C-PEPTIDE$^+$NKX6.1$^+$ in ISLC dispersed cells at day 33 on Transwell and Supragel conditions. (D) Immunofluorescence staining of C-PEPTIDE and GCG in ISLC on Transwell and Supragel conditions. Scale bar, 20 μm. (E) Quantification of the C-PEPTIDE$^+$ and GCG$^+$ cell aggregates at day 33 on the Supragel and in suspension conditions. n = 3–5 technical replicates. (F) and (G) Average ELISA measurements of secreted human insulin index in response to glucose challenge and total insulin content in ISLC on Transwell and Supragel conditions. n = 3 technical replicates. (H) Transmission electron micrographs of ISLC cultured on Transwell (left) and ISLC cultured on the Supragel (right), arrows indicated crystalline insulin granules. Scale bar, 1 μm. Data are shown in C as means ± SDs. ****: $p < 0.001$ and **: $p < 0.01$.

However, toward the end of stage 4 PP2 differentiation, the clusters likely rely more on the cell-cell interactions within each cell cluster, shown by elevated E-cadherin expression from the 5 mg/ml Supragel group (Fig. 4H and I). Our results are consistent with previous studies also showing increased mRNA expression of E-cadherin and N-CAM during hESC-DE differentiation toward the hESC-PP stage [31,57,58].

Regarding the mechanical properties of Supragel, matrix stiffness plays an important role on stem cell fate determination [36]. 2D matrix elasticity has been shown to be sufficient to direct MSC differentiation towards tissue-specific lineages [39]. For example, scaffolds of intermediate stiffness that mimic the skeletal muscle (8–17 kPa) tend to result in myogenic origin, while more rigid scaffolds that mimic bones (25–40 kPa) lead to MSC differentiation toward osteogenic [59]. In terms of neural stem cell, soft scaffolds with elastic modulus similar to the brain (0.1–1 kPa) can be neurogenic [60]. Our results shown that with the initial of differentiation the elastic modulus was ~0.8 kPa (for 2.5 mg/ml Supragel), 1.5 kPa (for 5 mg/ml Supragel) and 8 kPa (for 7.5 mg/ml Supragel). Neither 0.8 kPa nor 8 kPa, hPSCs appeared to be appropriate for induction toward the endoderm and pancreatic progenitors under the elastic modulus of 1.5 kPa, implicating a participating role of mechanic stiffness on pancreatic progenitor differentiation.

3.4. Generation of glucose-responsive islet-like cell clusters on Supragel

To obtain islet-like cell aggregates, we continued to induce PP2 aggregates into NKX6.1$^+$/NGN3$^+$ (Neurogenin 3, NGN3) endocrine progenitor cells (EPs; stage 5, S5) and NKX6.1$^+$/C-peptide$^+$ β-cells (stage 6, S6) with cell cultured on Matrigel or Supragel. At the end of S5, only ~25 % NKX6.1$^+$, ~7 % NGN3$^+$and ~5 % NKX6.1$^+$/NGN3$^+$ S5 cells of total cell populations were observed from the Matrigel group (Figs. S9A–C), which could be due to the less ideal stiffness provided by the polystyrene culture plastics [30]. In order to improve the differentiation efficiency, we transferred the PP2 cells into an air-liquid interface just before starting S5, as shown by previous studies [21]. As expected, the differentiation efficiency improved to ~40 % NKX6.1$^+$, ~20 % NGN3$^+$and ~10 % NKX6.1$^+$/NGN3$^+$ EP cells (Figs. S9C and S9D).

For cells maintained on Supragel, the cell clusters continued to be cultured on Supragel for the differentiation processes throughout S5 and S6, with additional supplement of growth factors (Fig. 6A). The differentiation efficiency for the Supragel group was significantly higher than the Matrigel/air-liquid interface group, giving percentages of ~60 % NKX6.1$^+$, ~40 % C-PEPTIDE$^+$, ~30 % NKX6.1$^+$/C-PEPTIDE$^+$ and ~5 % GCG$^+$ cells of total cell population (Fig. 6B,C and S9E).

Previous studies have reported that PP2 cells could differentiate into INS$^+$/GCG$^+$ double-positive polyhormonal cells, which are considered immature in β-cell differentiation [61]. We therefore further analyzed the expression of C-PEPTIDE and glucagon (GCG) and did not identify significant number of C-PEPTIDE$^+$/GCG$^+$ cells in the S6 clusters from the Supragel group (Fig. 6D and E). In vitro glucose-stimulated insulin secretion (GSIS) assay was also performed to verify the glucose responsiveness of these islet-like cells. As shown in Fig. 6F, the islet-like cell aggregates from the Supragel group showed significant elevation of insulin secretion in response to a high-concentration (16.7 mM) of glucose stimulus, as shown by insulin secretion index (amount of insulin secreted in 1.67 mM glucose divided by amount of insulin secreted in 16.7 mM glucose). The glucose-stimulated insulin secretory ability of the Supragel group was significantly better than cells from the Matrigel/air-liquid interface group (Fig. 6F), which failed to respond to high level glucose challenge (20.26 ng at 1.67 mM glucose per 100, 000 cells; 15.04 ng at 16.7 mM glucose per 100, 000 cells). Total insulin content of islet-like cell aggregates from the Supragel group was ~342 ng per 100,000 cells, also significantly more than the Matrigel/air-liquid interface group (Fig. 6G). Electron transmission microscopy (TEM) results showed the presence of insulin granules packaged within the insulin-producing β-cells generated from the Supragel group (Fig. 6H), all of which demonstrated the successful generation with better differentiation efficiency of islet-like cell clusters using Supragel.

Pancreatic islets are natural heterogeneous with sophisticated intra-islet cell-cell interaction and interaction between the islet cells with the surrounding ECM [62–64]. Extensive publications have also proven the crucial property of the exocrine ECM to the viability and physical function of the pancreatic islets [49,65,66]. The Supragel used here offered resemblance to that of exocrine ECM, and thus facilitated cell-ECM interaction during the early stages of hPSCs differentiation. Moreover, by promoting spontaneous hPSCs aggregation, the Supragel also encouraged cell-cell interactions within each cell clusters, both of above are necessary for pancreatic progenitor and insulin-secreting cell differentiation.

4. Conclusion

In summary, we report here a Supragel-based culture system for islet-like cluster differentiation. Supragel maintained stem cell viability and proliferation while facilitated spontaneous formation of hPSC into uniformed clusters by offering a suitable mechanical stiffness of ~1.5 kPa, as observed with multiple human pluripotent stem cell lines. Furthermore, by containing the RGD and YIGRS motifs, Supragel also provided appropriate cell adhesion sites, which enhanced Supragel-cell interaction via cell surface molecules such as integrin receptors and cadherins. These then resulted in an endoderm and their derivatives preferred differentiation by the Supragel-cultured hPSC as well as a more tolerance ability of the Supragel as a cell culture matrix, i.e., by being less dependent on the initial seeding density, without constant agitation and rotation during cell culture, and no requirement for the use of air/liquid interface culturing. Better differentiation efficiency was indeed observed from hPSCs maintained by Supragel into insulin-producing β-cells with excellent glucose-stimulated insulin secretion capacity. In summary, our data demonstrate that the Supragel-based culture system could provide an easy-to-use platform for the generation of insulin-secreting β-cells from the hPSCs.

Ethics approval and consent to participate

This study did not involve human or animal subjects. Thus, no ethical approval was required. The study protocol adhered to the guidelines established by the journal.

Data availability

The data that support the findings of this study are available from the corresponding author upon reasonable request.

CRediT authorship contribution statement

Hongmeng Ma: Writing – original draft, Methodology, Investigation, Data curation, Conceptualization. **Lilin Xu:** Writing – original draft, Methodology, Investigation, Data curation. **Shengjie Wu:** Methodology, Investigation, Data curation. **Songdi Wang:** Investigation, Data curation. **Jie Li:** Resources, Investigation, Data curation. **Sifan Ai:** Investigation, Data curation. **Zhuangzhuang Yang:** Methodology, Data curation. **Rigen Mo:** Investigation, Data curation. **Lei Lin:** Investigation. **Yan Li:** Investigation. **Shusen Wang:** Validation, Resources. **Jie Gao:** Writing – review & editing, Visualization, Validation, Funding acquisition. **Chen Li:** Writing – review & editing, Visualization, Validation, Funding acquisition. **Deling Kong:** Writing – review & editing, Supervision, Project administration, Funding acquisition, Conceptualization.

Declaration of competing interest

The authors declare that they have no known competing financial interests or personal relationships that could have appeared to influence

the work reported in this paper.

Acknowledgments

The work was supported by the National Key Technologies Research and Development Program of China (2020YFA0803701); the National Natural Science Foundation of China (81921004, T2122019); the CAMS Innovation Fund for Medical Sciences (2021–12M-1-052).

Appendix A. Supplementary data

Supplementary data to this article can be found online at https://doi.org/10.1016/j.bioactmat.2024.07.007.

References

[1] H.K. Kleinman, G.R. Martin, Matrigel: basement membrane matrix with biological activity, Semin. Cancer Biol. 15 (2005) 378–386, https://doi.org/10.1016/j.semcancer.2005.05.004.
[2] G. Rossi, A. Manfrin, M.P. Lutolf, Progress and potential in organoid research, Nat. Rev. Genet. 19 (2018) 671–687, https://doi.org/10.1038/s41576-018-0051-9.
[3] A. Marsee, F.J.M. Roos, M.M.A. Verstegen, H.P.B.O. Consortium, H. Gehart, E. de Koning, F. Lemaigre, S.J. Forbes, W.C. Peng, M. Huch, T. Takebe, L. Vallier, H. Clevers, L.J.W. van der Laan, B. Spee, Building consensus on definition and nomenclature of hepatic, pancreatic, and biliary organoids, Cell Stem Cell 28 (2021) 816–832, https://doi.org/10.1016/j.stem.2021.04.005.
[4] L. Huang, R. Desai, D.N. Conrad, N.C. Leite, D. Akshinthala, C.M. Lim, R. Gonzalez, L.B. Muthuswamy, Z. Gartner, S.K. Muthuswamy, Commitment and oncogene-induced plasticity of human stem cell-derived pancreatic acinar and ductal organoids, Cell Stem Cell 28 (2021) 1090–1104 e6, https://doi.org/10.1016/j.stem.2021.03.022.
[5] M. Breunig, J. Merkle, M. Wagner, M.K. Melzer, T.F.E. Barth, T. Engleitner, J. Krumm, S. Wiedenmann, C.M. Cohrs, L. Perkhofer, G. Jain, J. Kruger, P. C. Hermann, M. Schmid, T. Madacsy, A. Varga, J. Griger, N. Azoitei, M. Muller, O. Wessely, P.G. Robey, S. Heller, Z. Dantes, M. Reichert, C. Gunes, C. Bolenz, F. Kuhn, J. Maleth, S. Speier, S. Liebau, B. Sipos, B. Kuster, T. Seufferlein, R. Rad, M. Meier, M. Hohwieler, A. Kleger, Modeling plasticity and dysplasia of pancreatic ductal organoids derived from human pluripotent stem cells, Cell Stem Cell 28 (2021) 1105–1124 e19, https://doi.org/10.1016/j.stem.2021.03.005.
[6] N.C. Talbot, T.J. Caperna, Proteome array identification of bioactive soluble proteins/peptides in Matrigel: relevance to stem cell responses, Cytotechnology 67 (2015) 873–883, https://doi.org/10.1007/s10616-014-9727-y.
[7] S.S. Soofi, J.A. Last, S.J. Liliensiek, P.F. Nealey, C.J. Murphy, The elastic modulus of Matrigel as determined by atomic force microscopy, J. Struct. Biol. 167 (2009) 216–219, https://doi.org/10.1016/j.jsb.2009.05.005.
[8] E.A. Aisenbrey, W.L. Murphy, Synthetic alternatives to matrigel, Nat. Rev. Mater. 5 (2020) 539–551, https://doi.org/10.1038/s41578-020-0199-8.
[9] L.G. Villa-Diaz, H. Nandivada, J. Ding, N.C. Nogueira-de-Souza, P.H. Krebsbach, K. S. O'Shea, J. Lahann, G.D. Smith, Synthetic polymer coatings for long-term growth of human embryonic stem cells, Nat. Biotechnol. 28 (2010) 581–583, https://doi.org/10.1038/nbt.1631.
[10] G. Mondal, S. Barui, A. Chaudhuri, The relationship between the cyclic-RGDfK ligand and alphavbeta3 integrin receptor, Biomaterials 34 (2013) 6249–6260, https://doi.org/10.1016/j.biomaterials.2013.04.065.
[11] E.H. Nguyen, W.T. Daly, N.N.T. Le, M. Farnoodian, D.G. Belair, M.P. Schwartz, C. S. Lebakken, G.E. Ananiev, M.A. Saghiri, T.B. Knudsen, N. Sheibani, W.L. Murphy, Versatile synthetic alternatives to Matrigel for vascular toxicity screening and stem cell expansion, Nat. Biomed. Eng. 1 (2017), https://doi.org/10.1038/s41551-017-0096.
[12] M.K. Furue, J. Na, J.P. Jackson, T. Okamoto, M. Jones, D. Baker, R. Hata, H. D. Moore, J.D. Sato, P.W. Andrews, Heparin promotes the growth of human embryonic stem cells in a defined serum-free medium, Proc. Natl. Acad. Sci. U.S.A. 105 (2008) 13409–13414, https://doi.org/10.1073/pnas.0806136105.
[13] S. Musah, S.A. Morin, P.J. Wrighton, D.B. Zwick, S. Jin, L.L. Kiessling, Glycosaminoglycan-binding hydrogels enable mechanical control of human pluripotent stem cell self-renewal, ACS Nano 6 (2012) 10168–10177, https://doi.org/10.1021/nn3039148.
[14] Y.H. Tsou, J. Khoneisser, P.C. Huang, X. Xu, Hydrogel as a bioactive material to regulate stem cell fate, Bioact. Mater. 1 (2016) 39–55, https://doi.org/10.1016/j.bioactmat.2016.05.001.
[15] H. Donnelly, M. Salmeron-Sanchez, M.J. Dalby, Designing stem cell niches for differentiation and self-renewal, J. R. Soc. Interface 15 (2018), https://doi.org/10.1098/rsif.2018.0388.
[16] S. Koutsopoulos, S. Zhang, Long-term three-dimensional neural tissue cultures in functionalized self-assembling peptide hydrogels, matrigel and collagen I, Acta Biomater. 9 (2013) 5162–5169, https://doi.org/10.1016/j.actbio.2012.09.010.
[17] S.B. Anderson, C.C. Lin, D.V. Kuntzler, K.S. Anseth, The performance of human mesenchymal stem cells encapsulated in cell-degradable polymer-peptide hydrogels, Biomaterials 32 (2011) 3564–3574, https://doi.org/10.1016/j.biomaterials.2011.01.064.
[18] K. Gwon, E. Kim, G. Tae, Heparin-hyaluronic acid hydrogel in support of cellular activities of 3D encapsulated adipose derived stem cells, Acta Biomater. 49 (2017) 284–295, https://doi.org/10.1016/j.actbio.2016.12.001.
[19] M.R. Arkenberg, K. Koehler, C.C. Lin, Heparinized gelatin-based hydrogels for differentiation of induced pluripotent stem cells, Biomacromolecules 23 (2022) 4141–4152, https://doi.org/10.1021/acs.biomac.2c00585.
[20] Y. Du, Z. Liang, S. Wang, D. Sun, X. Wang, S.Y. Liew, S. Lu, S. Wu, Y. Jiang, Y. Wang, B. Zhang, W. Yu, Z. Lu, Y. Pu, Y. Zhang, H. Long, S. Xiao, R. Liang, Z. Zhang, J. Guan, J. Wang, H. Ren, Y. Wei, J. Zhao, S. Sun, T. Liu, G. Meng, L. Wang, J. Gu, T. Wang, Y. Liu, C. Li, C. Tang, Z. Shen, X. Peng, H. Deng, Human pluripotent stem-cell-derived islets ameliorate diabetes in non-human primates, Nat. Med. 28 (2022) 272–282, https://doi.org/10.1038/s41591-021-01645-7.
[21] A. Rezania, J.E. Bruin, P. Arora, A. Rubin, I. Batushansky, A. Asadi, S. O'Dwyer, N. Quiskamp, M. Mojibian, T. Albrecht, Y.H. Yang, J.D. Johnson, T.J. Kieffer, Reversal of diabetes with insulin-producing cells derived in vitro from human pluripotent stem cells, Nat. Biotechnol. 32 (2014) 1121–1133, https://doi.org/10.1038/nbt.3033.
[22] G.G. Nair, J.S. Liu, H.A. Russ, S. Tran, M.S. Saxton, R. Chen, C. Juang, M.L. Li, V. Q. Nguyen, S. Giacometti, S. Puri, Y. Xing, Y. Wang, G.L. Szot, J. Oberholzer, A. Bhushan, M. Hebrok, Recapitulating endocrine cell clustering in culture promotes maturation of human stem-cell-derived beta cells, Nat. Cell Biol. 21 (2019) 263–274, https://doi.org/10.1038/s41556-018-0271-4.
[23] D. Balboa, T. Barsby, V. Lithovius, J. Saarimaki-Vire, M. Omar-Hmeadi, O. Dyachok, H. Montaser, P.E. Lund, M. Yang, H. Ibrahim, A. Naatanen, V. Chandra, H. Vihinen, E. Jokitalo, J. Kvist, J. Ustinov, A.I. Nieminen, E. Kuuluvainen, V. Hietakangas, P. Katajisto, J. Lau, P.O. Carlsson, S. Barg, A. Tengholm, T. Otonkoski, Functional, metabolic and transcriptional maturation of human pancreatic islets derived from stem cells, Nat. Biotechnol. 40 (2022) 1042–1055, https://doi.org/10.1038/s41587-022-01219-z.
[24] J.R. Alvarez-Dominguez, J. Donaghey, N. Rasouli, J.H.R. Kenty, A. Helman, J. Charlton, J.R. Straubhaar, A. Meissner, D.A. Melton, Circadian entrainment triggers maturation of human in vitro islets, Cell Stem Cell 26 (2020) 108–122 e10, https://doi.org/10.1016/j.stem.2019.11.011.
[25] F.W. Pagliuca, J.R. Millman, M. Gurtler, M. Segel, A. Van Dervort, J.H. Ryu, Q. P. Peterson, D. Greiner, D.A. Melton, Generation of functional human pancreatic beta cells in vitro, Cell 159 (2014) 428–439, https://doi.org/10.1016/j.cell.2014.09.040.
[26] P.U. Mahaddalkar, K. Scheibner, S. Pfluger, Ansarullah, M. Sterr, J. Beckenbauer, M. Irmler, J. Beckers, S. Knobel, H. Lickert, Generation of pancreatic beta cells from CD177(+) anterior definitive endoderm, Nat. Biotechnol. 38 (2020) 1061–1072, https://doi.org/10.1038/s41587-020-0492-5.
[27] H. Liu, R. Li, H.K. Liao, Z. Min, C. Wang, Y. Yu, L. Shi, J. Dan, A. Hayek, L. Martinez Martinez, E. Nunez Delicado, J.C. Izpisua Belmonte, Chemical combinations potentiate human pluripotent stem cell-derived 3D pancreatic progenitor clusters toward functional beta cells, Nat. Commun. 12 (2021) 3330, https://doi.org/10.1038/s41467-021-23525-x.
[28] N.J. Hogrebe, K.G. Maxwell, P. Augsornworawat, J.R. Millman, Generation of insulin-producing pancreatic beta cells from multiple human stem cell lines, Nat. Protoc. 16 (2021) 4109–4143, https://doi.org/10.1038/s41596-021-00560-y.
[29] T. Barsby, H. Ibrahim, V. Lithovius, H. Montaser, D. Balboa, E. Vahakangas, V. Chandra, J. Saarimaki-Vire, T. Otonkoski, Differentiating functional human islet-like aggregates from pluripotent stem cells, STAR Protoc. 3 (2022) 101711, https://doi.org/10.1016/j.xpro.2022.101711.
[30] N.J. Hogrebe, P. Augsornworawat, K.G. Maxwell, L. Velazco-Cruz, J.R. Millman, Targeting the cytoskeleton to direct pancreatic differentiation of human pluripotent stem cells, Nat. Biotechnol. 38 (2020) 460–470, https://doi.org/10.1038/s41587-020-0430-6.
[31] J. Candiello, T.S.P. Grandhi, S.K. Goh, V. Vaidya, M. Lemmon-Kishi, K.R. Eliato, R. Ros, P.N. Kumta, K. Rege, I. Banerjee, 3D heterogeneous islet organoid generation from human embryonic stem cells using a novel engineered hydrogel platform, Biomaterials 177 (2018) 27–39, https://doi.org/10.1016/j.biomaterials.2018.05.031.
[32] H. Bi, K. Ye, S. Jin, Proteomic analysis of decellularized pancreatic matrix identifies collagen V as a critical regulator for islet organogenesis from human pluripotent stem cells, Biomaterials 233 (2020) 119673, https://doi.org/10.1016/j.biomaterials.2019.119673.
[33] R.L. Youngblood, J.P. Sampson, K.R. Lebioda, L.D. Shea, Microporous scaffolds support assembly and differentiation of pancreatic progenitors into beta-cell clusters, Acta Biomater. 96 (2019) 111–122, https://doi.org/10.1016/j.actbio.2019.06.032.
[34] S. Ai, H. Li, H. Zheng, J. Liu, J. Gao, J. Liu, Q. Chen, Z. Yang, A SupraGel for efficient production of cell spheroids, Sci. China Mater. 65 (2022) 1655–1661, https://doi.org/10.1007/s40843-021-1951-x.
[35] W. Lei, T. Feng, X. Fang, Y. Yu, J. Yang, Z.A. Zhao, J. Liu, Z. Shen, W. Deng, S. Hu, Signature of circular RNAs in human induced pluripotent stem cells and derived cardiomyocytes, Stem Cell Res. Ther. 9 (2018) 56, https://doi.org/10.1186/s13287-018-0793-5.
[36] K.H. Vining, D.J. Mooney, Mechanical forces direct stem cell behaviour in development and regeneration, Nat. Rev. Mol. Cell Biol. 18 (2017) 728–742, https://doi.org/10.1038/nrm.2017.108.
[37] C. Xu, M.S. Inokuma, J. Denham, K. Golds, P. Kundu, J.D. Gold, M.K. Carpenter, Feeder-free growth of undifferentiated human embryonic stem cells, Nat. Biotechnol. 19 (2001) 971–974, https://doi.org/10.1038/nbt1001-971.
[38] J. Zhang, S. Yun, Y. Du, A. Zannettino, H. Zhang, Hydrogel-based preparation of cell aggregates for biomedical applications, Appl. Mater. Today 20 (2020) 100747, https://doi.org/10.1016/j.apmt.2020.100747.

[39] A.J. Engler, S. Sen, H.L. Sweeney, D.E. Discher, Matrix elasticity directs stem cell lineage specification, Cell 126 (2006) 677–689, https://doi.org/10.1016/j.cell.2006.06.044.
[40] S. Gobaa, S. Hoehnel, M. Roccio, A. Negro, S. Kobel, M.P. Lutolf, Artificial niche microarrays for probing single stem cell fate in high throughput, Nat. Methods 8 (2011) 949–955, https://doi.org/10.1038/nmeth.1732.
[41] M.A. Baxter, M.V. Camarasa, N. Bates, F. Small, P. Murray, D. Edgar, S.J. Kimber, Analysis of the distinct functions of growth factors and tissue culture substrates necessary for the long-term self-renewal of human embryonic stem cell lines, Stem Cell Res. 3 (2009) 28–38, https://doi.org/10.1016/j.scr.2009.03.002.
[42] T.J. Rowland, L.M. Miller, A.J. Blaschke, E.L. Doss, A.J. Bonham, S.T. Hikita, L. V. Johnson, D.O. Clegg, Roles of integrins in human induced pluripotent stem cell growth on Matrigel and vitronectin, Stem Cell. Dev. 19 (2010) 1231–1240, https://doi.org/10.1089/scd.2009.0328.
[43] P. Zhou, B. Yin, R. Zhang, Z. Xu, Y. Liu, Y. Yan, X. Zhang, S. Zhang, Y. Li, H. Liu, Y. A. Yuan, S. Wei, Molecular basis for RGD-containing peptides supporting adhesion and self-renewal of human pluripotent stem cells on synthetic surface, Colloids Surf. B Biointerfaces 171 (2018) 451–460, https://doi.org/10.1016/j.colsurfb.2018.07.050.
[44] P. Pimton, S. Sarkar, N. Sheth, A. Perets, C. Marcinkiewicz, P. Lazarovici, P. I. Lelkes, Fibronectin-mediated upregulation of alpha5beta1 integrin and cell adhesion during differentiation of mouse embryonic stem cells, Cell Adhes. Migrat. 5 (2011) 73–82, https://doi.org/10.4161/cam.5.1.13704.
[45] D.A. Brafman, C. Phung, N. Kumar, K. Willert, Regulation of endodermal differentiation of human embryonic stem cells through integrin-ECM interactions, Cell Death Differ. 20 (2013) 369–381, https://doi.org/10.1038/cdd.2012.138.
[46] R.J. Slack, S.J.F. Macdonald, J.A. Roper, R.G. Jenkins, R.J.D. Hatley, Emerging therapeutic opportunities for integrin inhibitors, Nat. Rev. Drug Discov. 21 (2022) 60–78, https://doi.org/10.1038/s41573-021-00284-4.
[47] X. Pang, X. He, Z. Qiu, H. Zhang, R. Xie, Z. Liu, Y. Gu, N. Zhao, Q. Xiang, Y. Cui, Targeting integrin pathways: mechanisms and advances in therapy, Signal. Transduct. Target. Ther. 8 (2023) 1, https://doi.org/10.1038/s41392-022-01259-6.
[48] C. Zhang, Y. Shang, X. Chen, A.C. Midgley, Z. Wang, D. Zhu, J. Wu, P. Chen, L. Wu, X. Wang, K. Zhang, H. Wang, D. Kong, Z. Yang, Z. Li, X. Chen, Supramolecular nanofibers containing arginine-glycine-aspartate (RGD) peptides boost therapeutic efficacy of extracellular vesicles in kidney repair, ACS Nano 14 (2020) 12133–12147, https://doi.org/10.1021/acsnano.0c05681.
[49] A.E. Vlahos, S.M. Kinney, B.R. Kingston, S. Keshavjee, S.Y. Won, A. Martyts, W.C. W. Chan, M.V. Sefton, Endothelialized collagen based pseudo-islets enables tuneable subcutaneous diabetes therapy, Biomaterials 232 (2020) 119710, https://doi.org/10.1016/j.biomaterials.2019.119710.
[50] L. Li, S.A. Bennett, L. Wang, Role of E-cadherin and other cell adhesion molecules in survival and differentiation of human pluripotent stem cells, Cell Adhes. Migrat. 6 (2012) 59–70, https://doi.org/10.4161/cam.19583.
[51] A. Raza, C.S. Ki, C.C. Lin, The influence of matrix properties on growth and morphogenesis of human pancreatic ductal epithelial cells in 3D, Biomaterials 34 (2013) 5117–5127, https://doi.org/10.1016/j.biomaterials.2013.03.086.
[52] M. Bao, J. Cornwall-Scoones, E. Sanchez-Vasquez, A.L. Cox, D.Y. Chen, J. De Jonghe, S. Shadkhoo, F. Hollfelder, M. Thomson, D.M. Glover, M. Zernicka-Goetz, Stem cell-derived synthetic embryos self-assemble by exploiting cadherin codes and cortical tension, Nat. Cell Biol. 24 (2022) 1341–1349, https://doi.org/10.1038/s41556-022-00984-y.
[53] T.M. Brusko, H.A. Russ, C.L. Stabler, Strategies for durable beta cell replacement in type 1 diabetes, Science 373 (2021) 516–522, https://doi.org/10.1126/science.abh1657.
[54] J. Siehler, A.K. Blochinger, M. Meier, H. Lickert, Engineering islets from stem cells for advanced therapies of diabetes, Nat. Rev. Drug Discov. 20 (2021) 920–940, https://doi.org/10.1038/s41573-021-00262-w.
[55] J. Wu, M.R. Rostami, D.P. Cadavid Olaya, E.S. Tzanakakis, Oxygen transport and stem cell aggregation in stirred-suspension bioreactor cultures, PLoS One 9 (2014) e102486, https://doi.org/10.1371/journal.pone.0102486.
[56] E. Garreta, R.D. Kamm, S.M. Chuva de Sousa Lopes, M.A. Lancaster, R. Weiss, X. Trepat, I. Hyun, N. Montserrat, Rethinking organoid technology through bioengineering, Nat. Mater. 20 (2021) 145–155, https://doi.org/10.1038/s41563-020-00804-4.
[57] A.B. Prowse, F. Chong, P.P. Gray, T.P. Munro, Stem cell integrins: implications for ex-vivo culture and cellular therapies, Stem Cell Res. 6 (2011) 1–12, https://doi.org/10.1016/j.scr.2010.09.005.
[58] M. Brissova, M.J. Fowler, W.E. Nicholson, A. Chu, B. Hirshberg, D.M. Harlan, A. C. Powers, Assessment of human pancreatic islet architecture and composition by laser scanning confocal microscopy, J. Histochem. Cytochem. 53 (2005) 1087–1097, https://doi.org/10.1369/jhc.5C6684.2005.
[59] A.R. Cameron, J.E. Frith, J.J. Cooper-White, The influence of substrate creep on mesenchymal stem cell behaviour and phenotype, Biomaterials 32 (2011) 5979–5993, https://doi.org/10.1016/j.biomaterials.2011.04.003.
[60] J. Lam, S.T. Carmichael, W.E. Lowry, T. Segura, Hydrogel design of experiments methodology to optimize hydrogel for iPSC-NPC culture, Adv. Healthcare Mater. 4 (2015) 534–539, https://doi.org/10.1002/adhm.201400410.
[61] J.R. Millman, C. Xie, A. Van Dervort, M. Gurtler, F.W. Pagliuca, D.A. Melton, Generation of stem cell-derived beta-cells from patients with type 1 diabetes, Nat. Commun. 7 (2016) 11463, https://doi.org/10.1038/ncomms11463.
[62] G. Kesavan, O. Lieven, A. Mamidi, Z.L. Ohlin, J.K. Johansson, W.C. Li, S. Lommel, T.U. Greiner, H. Semb, Cdc42/N-WASP signaling links actin dynamics to pancreatic beta cell delamination and differentiation, Development 141 (2014) 685–696, https://doi.org/10.1242/dev.100297.
[63] D. Bosco, M. Armanet, P. Morel, N. Niclauss, A. Sgroi, Y.D. Muller, L. Giovannoni, G. Parnaud, T. Berney, Unique arrangement of alpha- and beta-cells in human islets of Langerhans, Diabetes 59 (2010) 1202–1210, https://doi.org/10.2337/db09-1177.
[64] M.P. Dybala, M. Hara, Heterogeneity of the human pancreatic islet, Diabetes 68 (2019) 1230–1239, https://doi.org/10.2337/db19-0072.
[65] T. Richardson, P.N. Kumta, I. Banerjee, Alginate encapsulation of human embryonic stem cells to enhance directed differentiation to pancreatic islet-like cells, Tissue Eng. 20 (2014) 3198–3211, https://doi.org/10.1089/ten.TEA.2013.0659.
[66] W. Wang, S. Jin, K. Ye, Development of islet organoids from H9 human embryonic stem cells in biomimetic 3D scaffolds, Stem Cell. Dev. 26 (2017) 394–404, https://doi.org/10.1089/scd.2016.0115.